Resonant stimulated Raman gain and loss spectroscopy in Rb atomic vapor

Liya Pei,[1] Xiaogang Lu,[1] Jinhai Bai,[1,2] Xingxu Miao,[1,3] Ruquan Wang,[1] Ling-An Wu,[1] Shiwei Ren,[2] Zhiyong Jiao,[3] Huafeng Zhu,[3] Panming Fu,[1,*] and Zhanchun Zuo[1,†]

[1]*Laboratory of Optical Physics, Beijing National Laboratory for Condensed Matter Physics, Institute of Physics, Chinese Academy of Sciences, Beijing 100190, China*

[2]*Hebei University of Science and Technology, Shijiazhuang, 050018, China*

[3]*China University of Petroleum East China–Qingdao Campus, Qingdao, 266580, China*

(Received 15 March 2013; published 14 June 2013)

Based on our experimental observations of the resonant stimulated Raman gain and loss spectra in Rb atomic vapor, we propose an alternative interpretation of electromagnetically induced transparency (EIT). We find that, in the presence of a coupling field, a probe beam can exhibit both gain and loss depending on the frequencies of the incident beams. The gain and loss can coexist in a Doppler-broadened system, leading to polarization interference between atoms of different velocities, with a sharp transition from gain to loss as the probe-field frequency is scanned. We use the concept of Raman gain, instead of the commonly accepted quantum Fano interference, to explain the phenomenon of EIT and its transparency window as being due to the suppression of linear absorption by the Raman gain. Using this concept, the phenomena of EIT and Autler-Townes splitting may be explained within the same framework.

DOI: 10.1103/PhysRevA.87.063822 PACS number(s): 42.65.Dr, 42.50.Gy

I. INTRODUCTION

Coherent Raman spectroscopy [1,2] is a powerful tool for studying the energy structure of atoms and molecules. There are various different techniques, but their common feature is that two incident beams with a frequency difference equal to the resonant frequency of the Raman mode are used to excite the Raman mode in the medium, which is then probed by one of the beams (or some other beam). For example, in stimulated Raman spectroscopy (SRS), we detect the change in intensity of the probe beam. Recently, coherent phenomena such as coherent population trapping [3], lasing without inversion [4], and electromagnetically induced transparency (EIT) [5,6] have attracted much attention. In particular, the latter phenomenon can eliminate absorption at a resonant frequency of a transition by applying a control field to another transition. The importance of EIT stems from the fact that it can enhance the nonlinear processes in the induced-transparency spectral region of the medium [7–10]. The transparency is also accompanied by steep dispersion, which has important applications in the field of quantum information processing [11–13].

There is a strong relationship between EIT and coherent Raman phenomena. Harris and co-workers used EIT to prepare near-maximal atomic coherence on a Raman transition in atomic Pb vapor, which they used to obtain highly efficient nonlinear frequency conversion [14]. They also utilized a type of strongly driven molecular coherence produced by EIT to generate ultrashort pulses of radiation [15,16]. Stimulated Raman scattering in EIT is another interesting phenomenon, which is important for its use in analyzing EIT [17]. On the other hand, Harada *et al.* [18] carried out a systematic study concerning the competition between EIT and stimulated Raman scattering.

In this paper, we shall study resonant stimulated Raman gain and loss spectroscopy in Rb atomic vapor. It is found that in the presence of a coupling field the probe beam can exhibit either gain or loss, depending on the frequencies of the incident beams. In a Doppler-broadened system, resonant transitions can be achieved through Doppler frequency shifting; thus gain and loss can coexist simultaneously, resulting in polarization interference between atoms of different velocities. In particular, due to the polarization interference, we observe a sharp transition from gain to loss as the frequency of the probe field is scanned.

Conventionally, EIT is explained as the result of quantum Fano interference. The requirement for this explanation is based on the fact that when the coupling field is very weak so that the Autler-Townes (AT) [19] doublet structure becomes overlapped, a sharp transmission window is still observable. Recently, Anisimov *et al.* [20] introduced a theoretical method based on the Akaikes information criterion to describe the transition from AT splitting to EIT as the pump power decreases. Relevant experimental tests were performed by Giner *et al.* [21]. In this paper, we use the concept of Raman gain and loss to explain EIT, which we show can be considered simply as the suppression of linear absorption by the Raman gain. Compared to quantum Fano interference, Raman gain is due to a real transition so it is conceptually simpler and more direct. Moreover, by using this model the phenomena of EIT and the AT effect may be explained within the same framework.

II. THEORY

A. Basic equations

Let us consider a Λ-type three-level system (Fig. 1), where the states between $|0\rangle$ and $|1\rangle$ and between $|1\rangle$ and $|2\rangle$ are coupled by dipolar transitions with resonant frequencies Ω_1 and Ω_2 and dipole moment matrix elements μ_1 and μ_2, respectively. A strong coupling field (beam 2) of frequency ω_2

*pmfu@iphy.ac.cn
†zczuo@iphy.ac.cn

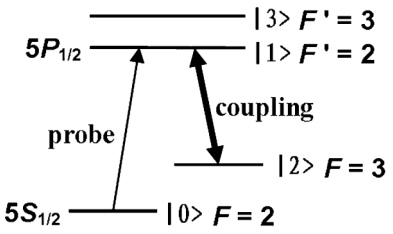

FIG. 1. Energy level diagram for ^{85}Rb.

resonantly couples the transition $|1\rangle$-$|2\rangle$, while a weak probe field (beam 1) of frequency ω_1 is applied to the transition $|0\rangle$-$|1\rangle$. At first, the simultaneous interactions of the atoms with beams 1 and 2 will induce atomic coherence between $|0\rangle$ and $|2\rangle$ through a two-photon transition. This atomic coherence then interacts further with the coupling field and thus changes the amplitude of the probe field.

Let the detunings be represented by $\Delta_i = \Omega_i - \omega_i$, so that after a canonical transformation the effective Hamiltonian becomes

$$H = \hbar\Delta_1|1\rangle\langle 1| + \hbar(\Delta_1 - \Delta_2)|2\rangle\langle 2| - [\mu_1 E_1|1\rangle\langle 0| + \mu_2 E_2|2\rangle\langle 1| + \text{H.c.}], \quad (1)$$

where E_1 and E_2 are the complex fields of the incident probe and coupling beams, respectively. The density matrix equation with relaxation terms included is given by

$$\frac{d\rho}{dt} = -\frac{i}{\hbar}[H,\rho] + \left(\frac{d\rho}{dt}\right)_{\text{relax}}, \quad (2)$$

in which the off-diagonal elements satisfy the following equations:

$$\begin{aligned}
\frac{d\rho_{10}}{dt} &= -(i\Delta_1 + \Gamma_{10})\rho_{10} + iG_2^*\rho_{20} + iG_1(\rho_{00} - \rho_{11}),\\
\frac{d\rho_{20}}{dt} &= -[i(\Delta_1 - \Delta_2) + \Gamma_{20}]\rho_{20} + iG_2\rho_{10} - iG_1\rho_{21}, \quad (3)\\
\frac{d\rho_{21}}{dt} &= (i\Delta_2 - \Gamma_{12})\rho_{21} - iG_1^*\rho_{20} - iG_2(\rho_{22} - \rho_{11}).
\end{aligned}$$

Here $G_i = \mu_i E_i/\hbar$ are the coupling coefficients, and Γ_{ij} is the transverse relaxation rate between states $|i\rangle$ and $|j\rangle$. The polarization at the frequency of the probe beam is $P_1 = N\mu_1\rho_{10}$, where N is the atomic density and the off-diagonal matrix element ρ_{10} is given by

$$\rho_{10} = \frac{i}{i\Delta_1 + \Gamma_{10}}[G_2^*\rho_{20} + G_1(\rho_{00} - \rho_{11})]. \quad (4)$$

The first term in Eq. (4) shows that the SRS arises from the Raman coherence ρ_{20}, while the second term corresponds to the linear absorption. Solving only to the first order in G_1 and under the condition $\rho_{11} \ll \rho_{00}, \rho_{22}$, we obtain

$$\rho_{20} = \frac{-G_1 G_2}{(i\Delta_1 + \Gamma_{10})[i(\Delta_1 - \Delta_2) + \Gamma_{20}] + |G_2|^2} \times \left(\rho_{00} - \frac{i\Delta_1 + \Gamma_{10}}{i\Delta_2 - \Gamma_{10}}\rho_{22}\right), \quad (5)$$

where $\Gamma_{12} = \Gamma_{10}$ is assumed.

B. Optical pumping effect

The populations ρ_{00} and ρ_{22} in Eq. (5) are strongly dependent on the coupling field. This optical pumping effect can be described by the following equations:

$$\begin{aligned}
\frac{d\rho_{00}}{dt} &= \Gamma\rho_{11} - \gamma\rho_{00} + \gamma'\rho_{22},\\
\frac{d\rho_{11}}{dt} &= -2\Gamma\rho_{11} - iG_2\rho_{12} + iG_2^*\rho_{21}, \quad (6)\\
\frac{d\rho_{22}}{dt} &= \Gamma\rho_{11} - \gamma'\rho_{22} + \gamma\rho_{00} + iG_2\rho_{12} - iG_2^*\rho_{21}.
\end{aligned}$$

Here, Γ denotes the decay rate from $|1\rangle$ to $|0\rangle$ (or $|2\rangle$), and γ (γ') is the relaxation rate from $|0\rangle$ to $|2\rangle$ ($|2\rangle$ to $|0\rangle$). Assuming $\Gamma \gg \gamma, \gamma'$, we obtain

$$\rho_{00} \simeq \frac{\gamma' + D|G_2|^2}{\gamma + \gamma' + D|G_2|^2}, \quad \rho_{22} \simeq \frac{\gamma}{\gamma + \gamma' + D|G_2|^2}, \quad (7)$$

where $D = \Gamma_{10}/(\Delta_2^2 + \Gamma_{10}^2)$.

Since we are interested in how the coupling field affects the propagation of the probe beam, in a real experiment we modulate the intensity of the coupling field, followed by demodulation of the probe beam, to obtain the induced gain or loss. As is well known, the coupling field can not only induce the Raman coherence but also cause redistribution of the population, thus affecting the linear absorption of the probe beam. This optical pumping effect can be investigated by calculating the change in population distribution in the presence of the coupling field, i.e., $\Delta\rho_{00} = \rho_{00}(|G_2|) - \rho_{00}(|G_2| = 0)$, which from Eq. (7) is found to be

$$\Delta\rho_{00} = \frac{\gamma D|G_2|^2}{(\gamma + \gamma')(\gamma + \gamma' + D|G_2|^2)}. \quad (8)$$

In summary, the change in the atomic polarization due to the presence of the coupling field is given by

$$\Delta P_1 = \frac{iN\mu_1}{i\Delta_1 + \Gamma_{10}}(G_2^*\rho_{20} + G_1\Delta\rho_{00}). \quad (9)$$

C. Resonant stimulated Raman spectroscopy

Now, we concentrate on studying the SRS in the case of a strong coupling field. For $D|G_2|^2 \gg \gamma$, we have $\rho_{00} \simeq 1$; therefore, from Eqs. (4) and (5) the polarization due to the SRS is given by

$$P_1^{\text{SRS}} = \frac{-iN\mu_1 G_1|G_2|^2}{(i\Delta_1 + \Gamma_{10})[i(\Delta_1 - \Delta_2) + \Gamma_{20}] + |G_2|^2} \times \frac{1}{i\Delta_1 + \Gamma_{10}}. \quad (10)$$

By solving for the pole in Eq. (10), i.e.,

$$(i\Delta_1 + \Gamma_{10})[i(\Delta_1 - \Delta_2) + \Gamma_{20}] + |G_2|^2 = 0, \quad (11)$$

we obtain

$$P_1^{\text{SRS}} = \frac{N\mu_1 G_1|G_2|^2}{(\Delta_1 - i\Gamma_{10})(\Delta_1 - \Delta_+)(\Delta_1 - \Delta_-)}. \quad (12)$$

Here,

$$\Delta_\pm = \tfrac{1}{2}[\Delta_2 + i(\Gamma_{10} + \Gamma_{20})] \pm \tfrac{1}{2}\sqrt{[\Delta_2 - i(\Gamma_{10} - \Gamma_{20})]^2 + 4|G_2|^2}. \quad (13)$$

Let us analyze the nature of the three poles in Eq. (12). The poles at $\Delta_\pm$ correspond to the transition from the ground state $|0\rangle$ to the two dressed states $|\pm\rangle$, which induces the Raman coherence ρ_{20}. On the other hand, according to Eq. (4) the pole at $\Delta_1 = i\Gamma_{10}$ indicates that after ρ_{20} is induced, the resonance for the atomic polarization $P_1^{\rm SRS}$ occurs at $\Delta_1 = 0$. These two types of poles have different characteristics. Let us consider the case of $\Delta_2 = 0$. For the resonance at $\Delta_1 = 0$, we have

$$P_1^{\rm SRS} = \frac{-iN\mu_1 G_1 |G_2|^2}{\Gamma_{10}(|G_2|^2 + \Gamma_{10}\Gamma_{20})}. \tag{14}$$

Since $\mathrm{Im}(P_1^{\rm SRS}) < 0$ the probe beam exhibits amplification. On the other hand, the resonances for the two dressed states occur at $\Delta_1 = \pm|G_2|$. In this case, we have

$$P_1^{\rm SRS} = \frac{N\mu_1 G_1 |G_2|^2 [i(|G_2|^2 - \Gamma_{10}\Gamma_{20}) - \Gamma_{10}|G_2|]}{\Gamma_{10}\left(|G_2|^2 + \Gamma_{10}^2\right)\left(|G_2|^2 + \Gamma_{20}^2\right)} \tag{15}$$

in the limit $\Gamma_{10} \gg \Gamma_{20}$. When $|G_2|^2 \gg \Gamma_{10}\Gamma_{20}$, we have $\mathrm{Im}(P_1^{\rm SRS}) > 0$ and the probe beam undergoes absorption. Physically, ρ_{20} is established through a two-photon transition from $|0\rangle$ to $|2\rangle$, so it requires absorption of a photon from the probe beam at a frequency $\Delta_1 = \pm|G_2|$ detuned from the one-photon resonance. On the other hand, after the Raman coherence ρ_{20} is induced, scattering of the coupling beam leads to the emission of an anti-Stokes photon, thus producing amplification of the probe beam at $\Delta_1 = 0$.

III. EXPERIMENT

The above theoretical analysis was verified by experiments with Rb atomic vapor at room temperature. As shown in Fig. 1, the probe and coupling lasers couple the $D1$ transition of ^{85}Rb from the hyperfine states $5S_{1/2}$, $F = 2$ ($|0\rangle$) and $5S_{1/2}$, $F = 3$ ($|2\rangle$) to the state $5P_{1/2}$, $F' = 2$ ($|1\rangle$), respectively. The decay rate of the $D1$ line is about 5.75 MHz, while the Doppler width at room temperature (27 °C) is about 510 MHz. On the other hand, there is another excited state $5P_{1/2}$, $F' = 3$ ($|3\rangle$) separated from $5P_{1/2}$, $F' = 2$ ($|1\rangle$) by about 361.6 MHz, which is within the Doppler width. This state does not change the physics of our experiment, but will affect the theoretical simulation of the spectrum, especially the optical pumping effect. Therefore, we shall use the actual level system to fit the experimental results.

The experimental setup is shown in Fig. 2. The optical fields were provided by two independent 795 nm diode lasers (DL1 and DL2), which had a linewidth of approximately 1 MHz. The beams from the probe and coupling lasers DL1 and DL2 were horizontally and vertically polarized, respectively. Both were coupled into optical fibers to improve their profiles, and then combined in a polarizing beam splitter (PBS) to propagate along the same direction. They were focused to spots approximately 0.3 and 0.7 mm in diameter, respectively, on the Rb vapor cell, which was 75 mm long. A polarizing beam splitter was used in front of the photodiode detector to eliminate the coupling field. An acousto-optic modulator (AOM) was employed to modulate the intensity of the coupling field, and a lock-in amplifier (LIA) to demodulate the probe field detected by the photodetector (PD).

In our experiments we locked the frequency of the coupling field while scanning the probe field. We considered the three cases of the coupling-field frequency (a) exactly on resonance, (b) detuned but still within the Doppler profile, and (c) far away from the Doppler profile. The intensity of the probe was kept at 2 μW throughout. Figure 3 shows the absorption of the probe beam as a function of Δ_1 when $\Delta_2 =$ (a) 0, (b) 390, and (c) 885 MHz, for a coupling-field intensity of 0.3, 1.5, and 6 mW, respectively. We note that here only the absorption induced by the coupling field could be measured. Also, due

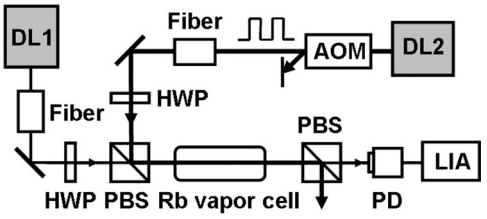

FIG. 2. Experimental setup. DL1 and DL2, diode lasers; PBS, polarizing beam splitter; HWP, half-wave plate; AOM, acousto-optic modulator; LIA, lock-in amplifier; PD, photodetector.

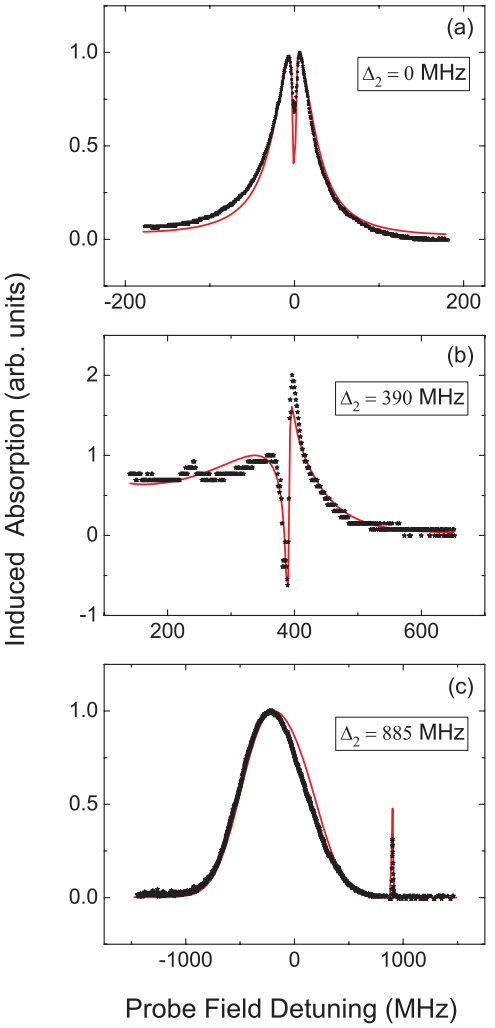

FIG. 3. (Color online) Experimental results for the induced absorption of the probe beam as a function of Δ_1 when $\Delta_2 =$ (a) 0, (b) 390, and (c) 885 MHz.

to the optical pumping effect, there exists a linear absorption profile in the spectrum. As shown in Fig. 3(a), there is a narrow transparent window at the center of the absorption profile when $\Delta_2 = 0$ MHz. On the other hand, as the frequency of the probe field is scanned, we observe a sharp transition from gain to loss in Fig. 3(b) when $\Delta_2 = 390$ MHz, which is within the Doppler profile. Finally, in Fig. 3(c), when Δ_2 is far away from the Doppler profile, i.e., $\Delta_2 = 885$ MHz, we observe two resonance absorption peaks with one very broad and the other much narrower than the Doppler width.

In the previous section we studied resonant SRS in a homogeneously broadened Λ-type three-level system. However, in a real experiment we need to consider the effects of Doppler broadening. In addition, the excited state $5P_{1/2}$, $F' = 3$ ($|3\rangle$) can also affect the theoretical simulation. The effects of Doppler broadening can be included easily, if we replace Δ_1 and Δ_2 by their Doppler-shift frequency detunings $\Delta_1^d = \Delta_1 - k_1 v$ and $\Delta_2^d = \Delta_2 - k_2 v$, respectively, and then integrate the induced polarization ΔP_1 given in Eq. (9) over the velocity distribution $W(\mathbf{v})$, where $\mathbf{v}$ is the atomic velocity, $W(\mathbf{v}) = (1/\sqrt{\pi}u)e^{-(v/u)^2}$ with $u = \sqrt{2KT/m}$, m is the mass of an atom, K the Boltzmann constant, and T the absolute temperature. On the other hand, due to the optical pumping, the involvement of the fourth level $5P_{1/2}$, $F' = 3$ can influence the absorption spectrum, in two aspects mainly. First, it can affect the population of the ground state, i.e., the term $\Delta\rho_{00}$ in Eq. (9). Second, since this state is separated from $|1\rangle$ by about 361.6 MHz, which is within the Doppler linewidth, it will affect the linear absorption profile. We use the following parameters to fit the experimental results: $\Gamma_{10} = 7.2$ MHz, $\Gamma_{20} = 0.72$ MHz, $\Gamma = 6$ MHz, and $\gamma = \gamma' = 0.12$ MHz. Here, we assume that $\gamma = \gamma'$ because $|0\rangle$ and $|2\rangle$ are the hyperfine states. The other parameters for Figs. 3(a), 3(b), and 3(c) are $\Delta_2 = 0$, 390, and 885 MHz, and $G_2 = 3.3$, 15, and 66 MHz, respectively. The solid curves in Figs. 3 are the theoretical curves. We see that the experimental results agree well with the theoretical fits. Finally, we discuss the effects of optical pumping on the SRS spectrum. For the case of $\Delta_2 = 0$, only atoms with velocity $v \simeq 0$ can be excited by the coupling field to the state $|1\rangle$, so the linear absorption profile in Fig. 3(a) is Doppler-free. By contrast, when Δ_2 is large, then all atoms can be excited to the state $|1\rangle$ or $|3\rangle$ through off-resonance excitation, leading to a very broad absorption spectrum at $\Delta_1 \simeq 0$, as shown in Fig. 3(c). Here, the involvement of the fourth level $|3\rangle$ strongly affects the position and linewidth of the spectrum.

IV. EFFECTS OF DOPPLER BROADENING ON THE SRS SPECTRUM BASED ON THE DRESSED-STATE MODEL

We have demonstrated experimentally that the spectrum of the induced absorption of the probe beam is strongly dependent on the detuning of the coupling field. To understand these spectra, in the following we shall neglect the effects of optical pumping and concentrate on analyzing the SRS spectrum in a Doppler-broadened system.

As mentioned before, SRS can give rise to either gain or loss in the probe beam depending on its frequency detuning. In a Doppler-broadened system the atoms can be in resonance with atomic states through Doppler frequency shifting; therefore, for a fixed frequency the probe field can be either absorbed or amplified depending on the atomic velocity. Specifically, in a Doppler-broadened system, the total susceptibility due to SRS is given by

$$P_T^{\mathrm{SRS}} = \int_{-\infty}^{\infty} d\mathbf{v}\, W(\mathbf{v}) P_1^{\mathrm{SRS}}(\mathbf{v}). \tag{16}$$

Here, $P_1^{\mathrm{SRS}}(\mathbf{v})$ is given by Eq. (10) with Δ_i replaced by the Doppler-shifted frequency detuning $\Delta_i^d = \Delta_i + \mathbf{k}_i \cdot \mathbf{v}$, where $\mathbf{k}_i$ is the wave vector of the ith beam. In our case, if beams 1 and 2 propagate along the same direction we have $k_1 \simeq k_2$, so

$$P_1^{\mathrm{SRS}}(v) = \frac{iN\mu_1 G_1 |G_2|^2/k_1^2}{[i(\Delta_1 - \Delta_2) + \Gamma_{20}](v - \tilde{v}_1)(v - \tilde{v}_2)}, \tag{17}$$

where

$$\tilde{v}_1 = \tilde{\Delta}_{10}, \quad \tilde{v}_2 = \tilde{\Delta}_{10} - \frac{|G_2|^2/k_1}{(\Delta_1 - \Delta_2) - i\Gamma_{20}}, \tag{18}$$

with $\tilde{\Delta}_{10} = (\Delta_1 - i\Gamma_{10})/k_1$.

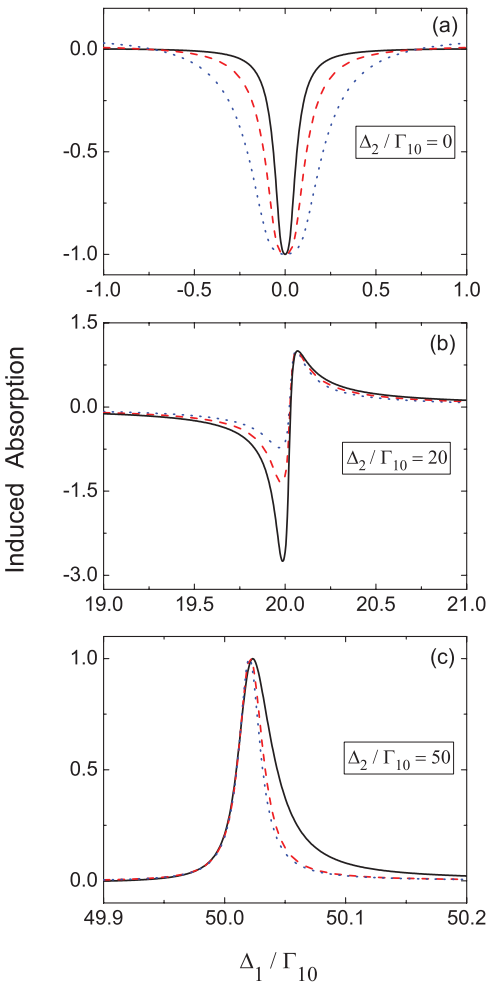

FIG. 4. (Color online) Numerical plots of the spectra of induced absorption in a Doppler-broadened Λ-type three-level system for Δ_2/Γ_{10} equal to (a) 0, (b) 20, and (c) 50, with $\Gamma_{10}/k_1 u = 0.05$ (solid curve), 0.1 (dashed curve), and 0.2 (dotted curve), for (a) and (c), and $\Gamma_{10}/k_1 u = 0.03$ (solid curve), 0.04 (dashed curve), and 0.05 (dotted curve) for (b). In (a) the minimum of $\mathrm{Im}[P_T^{\mathrm{SRS}}]$ is normalized to -1, while in (b) and (c) the maximum of $\mathrm{Im}[P_T^{\mathrm{SRS}}]$ is normalized to 1.

As shown in Eq. (17), there exist two poles in $P_1^{\mathrm{SRS}}(v)$. The pole at $\tilde{v}_1$ reflects the transition from $|0\rangle$ to $|1\rangle$, whereas that at $\tilde{v}_2$ is related to the resonance with the dressed state. Specifically, according to Eq. (13) of Ref. [22], the energies of the dressed states are given by

$$\varepsilon_{\pm}(v) = -\frac{k_1 v}{2} + \left(\Delta_1 - \frac{\Delta_2}{2}\right) \pm \frac{1}{2}\sqrt{(\Delta_2 - k_1 v)^2 + 4|G_2|^2} \tag{19}$$

for the Λ-type three-level system. Since the energy of the ground state $|0\rangle$ is 0, the resonance condition for the transition from the ground to the dressed state is $\varepsilon_{\pm}(v) = 0$, and we obtain the resonant velocity

$$v_2 = \Delta_{10} - \frac{|G_2|^2}{k_1(\Delta_1 - \Delta_2)}. \tag{20}$$

The above equation is exactly the same as Eq. (18) when relaxation rates are neglected. The values of $\tilde{v}_1$ and $\tilde{v}_2$ vary as we scan the probe beam, and the integral in Eq. (16) consists mainly of the contributions of atoms with velocities $v \simeq v_1$ and $v \simeq v_2$, where v_1 and v_2 are the real parts of $\tilde{v}_1$ and $\tilde{v}_2$, respectively. The atoms with velocities $v \simeq v_1$ and $v \simeq v_2$ will induce gain and loss for the probe beam, respectively.

We now present some numerical results for the SRS spectrum in a Doppler-broadened Λ-type three-level system with the parameters $\Gamma_{20}/\Gamma_{10} = 0.01$ and $G_2/\Gamma_{10} = 1$. Figure 4 shows the plots of the induced absorption spectra for values of Δ_2/Γ_{10} equal to (a) 0, (b) 20, and (c) 50; in Figs. 4(a) and 4(c) we have taken $\Gamma_{10}/k_1 u = 0.05$ (solid curve), 0.1 (dashed curve), and 0.2 (dotted curve); in Fig. 4(b), $\Gamma_{10}/k_1 u = 0.03$ (solid curve), 0.04 (dashed curve), and 0.05 (dotted curve). As shown in Fig. 4(a), when $\Delta_2/\Gamma_{10} = 0$ the SRS spectrum exhibits a narrow gain, which becomes narrower as the Doppler linewidth increases. On the other hand, there is a transition from gain to loss when Δ_2 is tuned within the Doppler profile [Fig. 4(b)]. When Δ_2 extends beyond the Doppler profile [see Fig. 4(c)], we observe an asymmetric absorption peak with a linewidth much narrower than the Doppler width at $\Delta_1 \simeq \Delta_2$. In contrast to the case of $\Delta_2 = 0$, the resonant peak becomes broader as the Doppler linewidth increases. These numerical results are consistent with the experimental results shown in Fig. 3. We note that in Fig. 3(c) the broad resonant peak at $\Delta_1 \simeq 0$ observed experimentally for $\Delta_2 = 885$ MHz is due to the optical pumping effect.

The frequency dependence of the SRS spectrum can be explained by the dressed-state model. Figure 5(a), 6(a), and 7(a) present the imaginary parts of $P_1^{\mathrm{SRS}}(v)$ for $\Delta_2/\Gamma_{10} = 0$, 20, and 50, respectively, when $\Gamma_{10}/k_1 u = 0.05$. In Fig. 5(a), $\Delta_1/\Gamma_{10} = 0$ (solid curve), 0.05 (dashed curve), 0.1 (dotted curve), and 0.5 (dash-dotted curve); in Fig. 6(a), $\Delta_1/\Gamma_{10} = 20$ (solid curve), 20.03 (dashed curve), 20.05 (dotted curve), and 20.3 (dash-dotted curve); in Fig. 7(a), $\Delta_1/\Gamma_{10} = 50$ (solid curve), 50.02 (dashed curve), 50.04 (dotted curve), and 50.06 (dash-dotted curve). On the other hand, Figs. 5(b), 6(b), and 7(b) present the corresponding resonant velocities v_1/u (dotted curve) and v_2/u (solid curve) as functions of Δ_1/Γ_{10}.

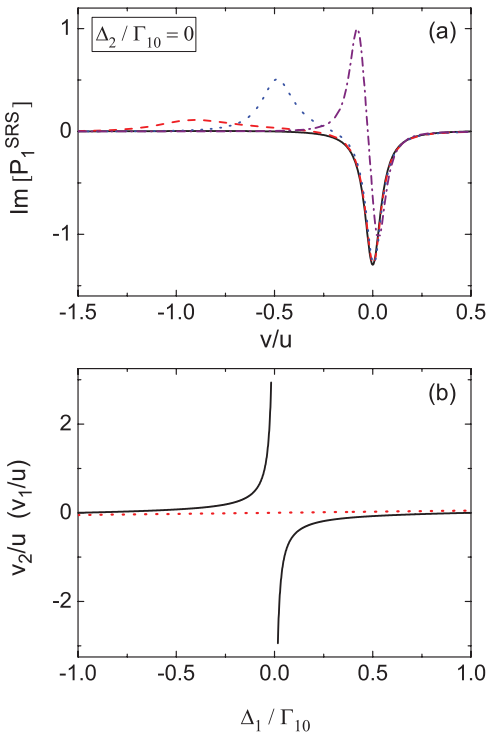

FIG. 5. (Color online) (a) Imaginary part of $P_1^{\mathrm{SRS}}(v)$ for $\Delta_2/\Gamma_{10} = 0$ when $\Gamma_{10}/k_1 u = 0.05$, with $\Delta_1/\Gamma_{10} = 0$ (solid curve), 0.05 (dashed curve), 0.1 (dotted curve), and 0.5 (dash-dotted curve). (b) Corresponding resonant velocities v_1/u (dotted curve) and v_2/u (solid curve) as functions of Δ_1/Γ_{10}. In (a) the maximum of $\mathrm{Im}[P_1^{\mathrm{SRS}}(v)]$ with $\Delta_1/\Gamma_{10} = 0.5$ is normalized to 1.

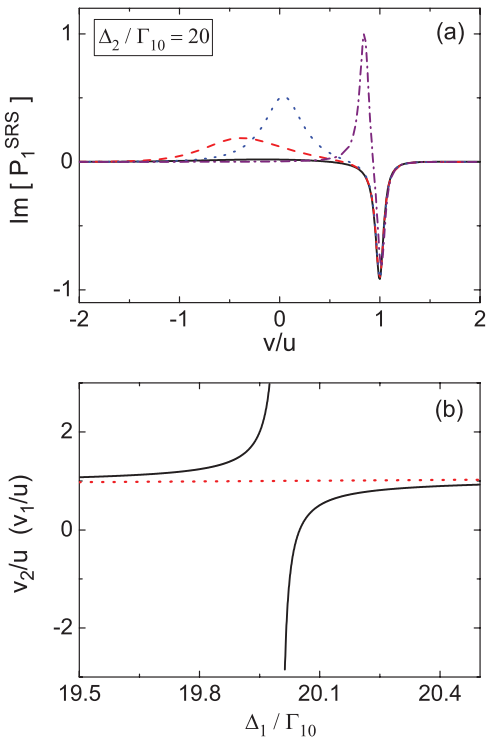

FIG. 6. (Color online) (a) Imaginary part of $P_1^{\mathrm{SRS}}(v)$ for $\Delta_2/\Gamma_{10} = 20$ when $\Gamma_{10}/k_1 u = 0.05$, with $\Delta_1/\Gamma_{10} = 20$ (solid curve), 20.03 (dashed curve), 20.05 (dotted curve), and 20.3 (dash-dotted curve). (b) Corresponding resonant velocities v_1/u (dotted curve) and v_2/u (solid curve) as functions of Δ_1/Γ_{10}. In (a) the maximum of $\mathrm{Im}[P_1^{\mathrm{SRS}}(v)]$ with $\Delta_1/\Gamma_{10} = 20.3$ is normalized to 1.

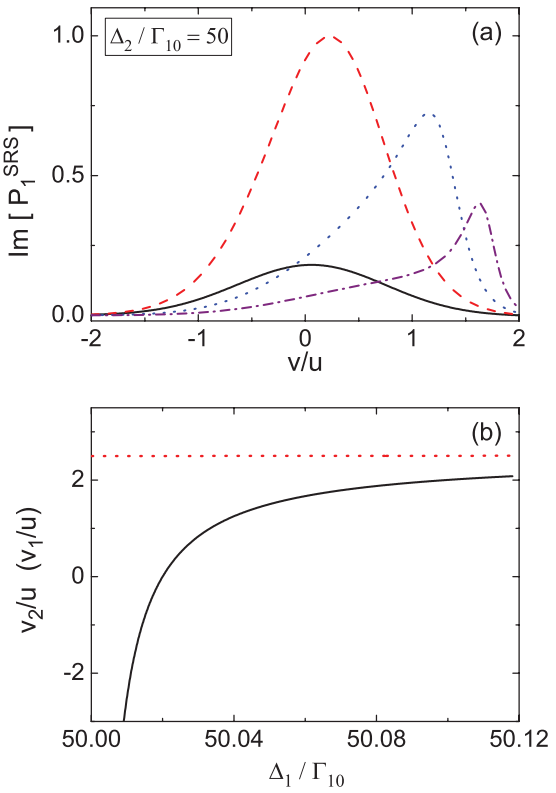

FIG. 7. (Color online) (a) Imaginary part of $P_1^{\rm SRS}(v)$ for $\Delta_2/\Gamma_{10}=50$ when $\Gamma_{10}/k_1u=0.05$, with $\Delta_1/\Gamma_{10}=50$ (solid curve), 50.02 (dashed curve), 50.04 (dotted curve), and 50.06 (dash-dotted curve). (b) Corresponding resonant velocities v_1/u (dotted curve) and v_2/u (solid curve) as functions of Δ_1/Γ_{10}. In (a) the maximum of $\mathrm{Im}[P_1^{\rm SRS}(v)]$ with $\Delta_1/\Gamma_{10}=50.02$ is normalized to 1.

Now we examine the frequency dependence of the resonant velocities shown in Figs. 5(b), 6(b), and 7(b). According to Eq. (18), $|v_2/u|\to\infty$ when $\Delta_1=\Delta_2$, so no atom in the Doppler profile can be in resonance with the dressed state. On the other hand, when Δ_1 is far from Δ_2 then we have $v_2\simeq v_1$, causing almost complete cancellation of the contributions from the two poles.

Let us first consider the case of $\Delta_2/\Gamma_{10}=0$, which shows a narrow gain [Fig. 4(a)]. When $\Delta_1/\Gamma_{10}=0$, $\mathrm{Im}[P_1^{\rm SRS}(v)]$ exhibits a single dip [solid curve in Fig. 5(a)] due to the pole at $\tilde{v}_1$. As Δ_1 is tuned away from the resonance, atoms with velocity v_2 will be in resonance with one of the dressed states, and thus destructive interference between contributions from the poles $\tilde{v}_1$ and $\tilde{v}_2$ causes the signal of $P_T^{\rm SRS}$ to decrease. The width of the narrow gain $\Gamma_{\rm SRS}$ can be estimated by assuming $v_2\simeq u$ so that there is effective cancellation between the contributions from these two poles. We obtain $\Gamma_{\rm SRS}=|G_2|^2/k_1u$, indicating that the SRS signal narrows as the Doppler linewidth increases.

Destructive polarization interference can also be employed to explain the spectrum of $\Delta_2/\Gamma_{10}=20$ [Fig. 4(b)]. Here again, due to the absence of the resonance from the pole at $\tilde{v}_2$, $\mathrm{Im}[P_1^{\rm SRS}(v)]$ exhibits a single dip [solid curve in Fig. 6(a)] when $\Delta_1/\Gamma_{10}=20$. On the other hand, when Δ_1 is tuned to the point where v_2 is near the center of the Doppler profile [dotted curve in Fig. 6(a) with $\Delta_1/\Gamma_{10}=20.05$], then because more atoms contribute to the signal, the spectrum shows a transition from gain to loss. The peak of the loss can be estimated by assuming that $v_2/u=0$, for which we obtain $\Delta_1\simeq\Delta_2+|G_2|^2/\Delta_2$. Finally, let us consider the case of $\Delta_2/\Gamma_{10}=50$, far away from the Doppler profile. Since there is no contribution from the pole at $\tilde{v}_1$ when $\Delta_1\simeq\Delta_2$, the spectrum is purely absorptive [Fig. 4(c)]. Specifically, no atom can be in resonance with the dressed state when $\Delta_1/\Gamma_{10}=50$ [see Fig. 7(b)], and thus $\mathrm{Im}[P_1^{\rm SRS}(v)]$ is relatively small [solid curve in Fig. 7(a)]. The amplitude of $\mathrm{Im}[P_1^{\rm SRS}(v)]$ increases to its maximum as Δ_1 is tuned to the frequency $\Delta_2+|G_2|^2/\Delta_2$ at which point $v_2/u=0$ [dashed curve in Fig. 7(a)], and then decreases as v_2/u moves out of the Doppler profile [dotted and dash-dotted curves in Fig. 7(a)]. This also explain why the spectrum is asymmetric.

V. DISCUSSION AND CONCLUSION

So far, we have discussed resonant stimulated Raman gain and loss spectroscopy in Rb atomic vapor. Now let us compare SRS with EIT. In EIT, we measure the absorption of a probe beam in the presence of a coupling field. By contrast, the SRS spectrum is obtained through demodulation of the probe beam when the coupling field is modulated. Thus, the SRS spectrum will convert to the EIT spectrum if the linear absorption term is included. From the theoretical viewpoint, by setting $\rho_{00}=1$ and $\rho_{11}=\rho_{22}=0$, from Eqs. (4) and (5) we obtain

$$P_1=\frac{iN\mu_1G_1[i(\Delta_1-\Delta_2)+\Gamma_{20}]}{(i\Delta_1+\Gamma_{10})[i(\Delta_1-\Delta_2)+\Gamma_{20}]+|G_2|^2}. \quad (21)$$

This expression is exactly the same as that for EIT [5,6], and similar spectra have indeed been observed in EIT experiments [23]. From the physical viewpoint that we have presented above, it is the suppression of linear absorption by Raman gain that leads to EIT. Compared to the conventional explanation of EIT being due to quantum Fano interference, since Raman gain originates from a real transition, our interpretation is more direct.

Using our theory, we can explain the phenomena of EIT and AT splitting within the same framework. As is well known, both phenomena can give rise to transparency in an absorption profile. On the other hand, only EIT can produce strong transparency with a very weak coupling field. Previously, this was widely considered to be the result of quantum Fano interference. Without interference, the transparency is simply due to a doublet structure in the absorption profile, i.e., AT splitting.

Our idea of Raman gain and loss can be used to establish the interrelation between EIT and AT splitting. It is different from previous works in that both effects can be considered as the same phenomenon in different regimes. Let us consider a homogeneously broadened system. Also, for simplicity here we consider the case of $\Delta_2=0$. First, the Raman coherence ρ_{20} is induced through the transition from $|0\rangle$ to the dressed states by the absorption of photons from the probe beam. Further interaction of the Raman coherence with the coupling field leads to the emission of anti-Stokes photons at the frequency of the probe beam. The resonant frequencies of these two processes are quite different. For the case of a strong coupling field, i.e., $|G_2|>\Gamma_{10}$, the transition to the dressed states is well separated from the transition to the state $|1\rangle$. In the

frequency range $|\Delta_1| \leqslant \Gamma_{10}$, according to Eq. (10), we have $P_1^{\mathrm{SRS}} = -iN\mu_1 G_1/(i\Delta_1 + \Gamma_{10})$ in the limit of $|G_2| \gg \Gamma_{10}$. Thus, the amplification of the probe beam due to the Raman gain cancels the linear absorption completely, and we observe AT splitting in the absorption spectrum. In the case of a weak coupling field, when the AT doublets are not well separated, the Raman gain at $\Delta_1 = 0$ leads to a transparency window in the absorption spectrum. This window is bounded by the enhanced absorption from the transition to the dressed state at $|\Delta_1| = |G_2|$. Since the separation between two dressed states can be very small for a weak coupling field, we obtain a sharp EIT window.

Finally, in this paper we have demonstrated the importance of the effect of optical pumping in the SRS spectrum. The optical pumping involves the transition of the population from the state $|2\rangle$ to the state $|0\rangle$ under a strong coupling field; therefore, it depends on the initial population of the state $|2\rangle$. According to Eq. (7), when $G_2 = 0$ we have $\rho_{22}/\rho_{00} = \gamma/\gamma'$ with $\gamma' \geqslant \gamma$ in general. If $|0\rangle$ and $|2\rangle$ are hyperfine structures, then $\gamma \simeq \gamma'$, and we have $\rho_{00} \simeq \rho_{22} \simeq 1/2$. In this case, accompanying the Raman gain or loss, there exists linear absorption of the probe beam due to the optical pumping effect. By contrast, if $\gamma' \gg \gamma$ then we have $\rho_{22} \simeq 0$, and therefore there will be no optical pumping effect. Specifically, we have $\Delta\rho_{00} \simeq 0$ according to Eq. (8). In this case, the change in the atomic polarization due to the presence of the coupling field originates solely from the Raman coherence ρ_{20} and we obtain a pure SRS spectrum as a result. This can happen in molecular systems, where $|2\rangle$ has negligible population and thus all the particles are in the state $|0\rangle$ initially.

In conclusion, we have studied resonant stimulated Raman gain and loss spectroscopy in Rb atomic vapor. It is found that when the probe beam is in resonance with the $|0\rangle$-$|1\rangle$ transition it will acquire gain. On the other hand, if the probe beam induces a transition from $|0\rangle$ to the dressed states, then absorption occurs. In a Doppler-broadened system, these resonant transitions can be achieved through Doppler frequency shifting; as a result, gain and loss can coexist, leading to polarization interference between atoms of different velocities. In particular, a sharp transition from gain to loss occurs as the frequency of the probe field is scanned. The concept of Raman gain can also be employed instead of quantum interference to interpret the phenomenon of EIT. Specifically, the sharp transparent window in EIT can be explained as being due to the suppression of linear absorption by the Raman gain. Using this concept, we can explain the phenomena of EIT and AT splitting within the same framework.

ACKNOWLEDGMENTS

The authors acknowledge financial support from the National Natural Science Foundation of China under Grants No. 10974252, No. 11274376, and No. 60978002, the National Basic Research Program of China, Grant No. 2010CB922904, and the National High Technology Research and Development Program of China, Grant No. 2011AA120102.

[1] G. L. Eesley, *Coherent Raman Spectroscopy* (Pergamon, Oxford, 1981).
[2] Y. R. Shen, *The Principles of Nonlinear Optics* (John Wiley & Sons, New York, 1984).
[3] E. Arimondo, *Coherent Population Trapping in Laser Spectroscopy*, Progress in Optics Vol. 5 (Elsevier, Amsterdam, 1996), pp. 257–354.
[4] O. Kocharovskaya, Phys. Rep. **219**, 175 (1992).
[5] S. E. Harris, Phys. Today **50**(7), 36 (1997).
[6] M. Fleischhauer, A. Imamoglu, and J. P. Marangos, Rev. Mod. Phys. **77**, 633 (2005).
[7] H. Kang and Y. Zhu, Phys. Rev. Lett. **91**, 093601 (2003).
[8] H. Wang, D. Goorskey, and M. Xiao, Phys. Rev. Lett. **87**, 073601 (2001).
[9] Z.-B. Wang, K.-P. Marzlin, and B. C. Sanders, Phys. Rev. Lett. **97**, 063901 (2006).
[10] Z. Zuo, J. Sun, X. Liu, Q. Jiang, G. Fu, L.-A. Wu, and P. Fu, Phys. Rev. Lett. **97**, 193904 (2006).
[11] M. Fleischhauer and M. D. Lukin, Phys. Rev. Lett. **84**, 5094 (2000).
[12] C. Liu, Z. Dutton, C. H. Behroozi, and L. V. Hau, Nature (London) **409**, 490 (2001).
[13] D. F. Phillips, A. Fleischhauer, A. Mair, R. L. Walsworth, and M. D. Lukin, Phys. Rev. Lett. **86**, 783 (2001).
[14] M. Jain, H. Xia, G. Y. Yin, A. J. Merriam, and S. E. Harris, Phys. Rev. Lett. **77**, 4326 (1996).
[15] S. E. Harris and A. V. Sokolov, Phys. Rev. Lett. **81**, 2894 (1998).
[16] D. D. Yavuz, D. R. Walker, M. Y. Shverdin, G. Y. Yin, and S. E. Harris, Phys. Rev. Lett. **91**, 233602 (2003).
[17] M. M. Kash, V. A. Sautenkov, A. S. Zibrov, L. Hollberg, G. R. Welch, M. D. Lukin, Y. Rostovtsev, E. S. Fry, and M. O. Scully, Phys. Rev. Lett. **82**, 5229 (1999).
[18] K. I. Harada, T. Kanbashi, M. Mitsunaga, and K. Motomura, Phys. Rev. A **73**, 013807 (2006).
[19] S. H. Autler and C. H. Townes, Phys. Rev. **100**, 703 (1955).
[20] P. M. Anisimov, J. P. Dowling, and B. C. Sanders, Phys. Rev. Lett. **107**, 163604 (2011).
[21] L. Giner, L. Veissier, B. Sparkes, A. S. Sheremet, A. Nicolas, O. S. Mishina, M. Scherman, S. Burks, I. Shomroni, D. V. Kupriyanov, P. K. Lam, E. Giacobino, and J. Laurat, Phys. Rev. A **87**, 013823 (2013).
[22] J. Niu, L. Pei, X. Lu, R. Wang, L.-A. Wu, and P. Fu, Phys. Rev. A **84**, 033853 (2011).
[23] J. Gea-Banacloche, Y. Q. Li, S. Z. Jin, and M. Xiao, Phys. Rev. A **51**, 576 (1995).